The 12th International Conference of
International Association for Computer Methods and Advances in Geomechanics (IACMAG)
1-6 October, 2008
Goa, India

Modelling of Desiccation Crack Development in Clay Soils

Susanga Costa, Jayantha Kodikara,
Department of Civil Engineering, Monash University, Australia

N. I. Thusyanthan
Schofield Centre, Department of Engineering, University of Cambridge, UK

Keywords: desiccation cracks, PIV analysis, crack initiation

ABSTRACT: Desiccation cracking can pose severe detrimental effects on the performance of clayey soils or generally of geomaterials in various engineering applications. Some examples of such applications include compacted clay barriers in waste containment, dam cores, canal liners, shallow foundations, buried pipelines and road pavements. Currently, there is no general method for modelling the desiccation crack development process, and the overall process is poorly understood. This paper presents explanations of crack evolution on the basis of laboratory desiccation tests using time-lapse photography and PIV analysis. Relationships between desiccation rate, average cell area, and specimen thickness are examined and discussed.

1 Introduction

Clay soils produce shrinkage cracks during desiccation. Evaporation of water from soil surface gives rise to restrained shrinkage, which in turn generates tensile stresses leading to shrinkage cracks as stresses exceed the material strength. This is a very complex phenomenon due to the interactions that take place during the process among material, ambience, and boundary conditions. For instance, as the soil water content decreases, soil material properties will change affecting the rate of moisture flow and water evaporation, soil tensile strength, modulus and fracture toughness, and the boundary adhesion. Thus, understanding and modelling of the cracking process has been poorly developed.

The presence of cracks significantly affects the performance of clay soils in various geoengineering applications. Some examples of such applications include compacted clay barriers in waste containment, dam cores, canal liners, shallow foundations, buried pipelines and road pavements. Other disciplines, such as agricultural engineering, mining engineering and materials engineering have also been affected by shrinkage cracks. In agricultural engineering, cracks can influence the water and solute flow through soil in irrigated land. A substantial amount of research work has been conducted in materials engineering on this issue to study the glazing and thermal fracturing in ceramics (e.g. Chiu & Cima, 1993) and printing, painting & washing (e.g. Deegan et al., 1997).

Majority of the previous studies on desiccation cracking were focused on the qualitative behaviour of cracks (Kodikara et al., 2000; Muller, 1998), excepting few exceptions that considered theoretical modelling (e.g., Peron et al, 2007; Kodikara and Choi, 2006; Konrad and Ayad, 1997; Morris et al., 1992; Lachenbruch, 1961). Furthermore, many researchers have tended to work on the final state of the cracked material (Morris et al, 1992; Kodikara et al, 2000; Yesiller et al., 2000). In view of modelling the cracking process, it is more important to understand the complete picture behind the crack evolution as well as the propagation. Some researchers (Nahlawi and Kodikara, 2006; Lakshmikantha, 2007) presented results of cracking tests giving details on the onset of first crack, cracking water content and subsequent crack evolution. Costa and Kodikara (2007) used the time-lapsed photography to capture the complete cracking process, and produced a series of video-clips for crack evolution. On the basis of this evidence, they highlighted some important mechanics of the crack evolution. They highlighted that the desiccation cracking process in clay is primarily influenced by subdivision due to stress concentration, where the actual subdivision locations are controlled by the activated flaws within the material. Costa et al., (2008) further indicated that Particle Image Velocimetry (PIV) technique could be a useful tool in analysing stress and stress distribution during cracking. In this paper, we present the results of thin layer desiccation cracking tests which were analysed using the PIV technique and discuss the different relationship governing crack evolution.

2 Material

Werribee clay was used for the tests described in this paper. This soil was available at the Aquatic Centre construction site located in Werribee, about 26 kilometres west of Melbourne. The samples were obtained at a depth of 1.5m – 2.0m from the surface. Werribee clay has been classified as a highly reactive soil featuring high shrink/swell potential. . More details of this clay may be found in a number of publications (e.g., Nahlawi, 2004; Nahlawi and Kodikara, 2006). Some basic properties of this soil are given in Table 1.

Table 1. Properties of Werribee Clay

Property	Value
Liquid Limit	127%
Plastic Limit	26%
Plasticity Index	101
Specific gravity	2.66
Linear Shrinkage	22%
Colour	Gray

3 Experimental Procedure

Werribee clay was oven dried, crushed and sieved and the component passing 425µm was used for preparing specimens. Processed clay was mixed with water close to its liquid limit and cured for 24 hours until the moisture was homogenised. The soil specimens were prepared by manually placing soil into moulds using a spatula without additional compaction effort. In order to avoid adhesion of the soil to the sidewalls of the moulds, the sidewalls were slightly greased prior to the soil placement. However, the base was not greased allowing for full adhesion to take place between the soil and the metal mould. During soil placement, the moulds were tapped carefully to release any entrapped air. Red sand particles were randomly distributed over the surface in order to acquire adequate texture required for the PIV analysis.

Rectangular metal moulds were used with three different thicknesses; 10, 20 and 30mm. The dimensions of the three moulds were 600 x 25 x 10 mm, 600 x 25 x 20 mm and 600 x 25 x 30mm. Specimens were kept on an electronic balance, which measured and recorded the weight of the specimen at regular intervals. A plastic sheet containing target markers was placed between the balance and the specimen which is necessary for PIV analysis. A digital camera was mounted on top of the set up which captured and saved the images at 5min intervals. A flood light was used to gain the sufficient light needed for better pictures. The temperature and relative humidity of the ambient conditions close to the moulds were measured during testing, and both these parameters remained reasonably constant. Specimen were continued to dry for about 72 hours. The initial and final moisture contents were measured using oven dried samples. Details are given in Table 2.

Table 2. Summary of the tests

Test No.	Mould Dimensions / (mm)	Surrounding Temperature / (C^0)	Relative Humidity / (%)	Initial Moisture content / (%)	Dry Density / (kg/m^3)
1	600 x 25 x 10	25	40	126	749.5
2	600 x 25 x 20	26	43	130	615.5
3	600 x 25 x 30	25	38	127	631.6

4 PIV analysis

Particle Image Velocimetry (PIV) analysis has been used in recent years to study failure mechanisms and strain fields in soil mechanics problems (White, 2002; White et al., 2003). Thusyanthan, et al. 2007 has successfully incorporated this technique to study the crack initiation during flexure of beams of clay. The theory and the procedure of the PIV technique is described in detail in above mentioned literature. The PIV analysis essentially involves computer analysis of pixel movement between pictures with respect to target textural properties of the surface, resulting in strains and displacement fields on the material surface. In contrast to tracking of target markers placed on an observation surface, this method relies on the computer textural analysis of the observation surface to compute strains and displacements. However, a calibration procedure is required to convert pixel movement to actual displacement units such as millimetres.

Presentation of results

The results of the tests are presented in both graphical and statistical forms. Figure 1 illustrates the final crack patterns in the three specimens. Sequential subdivision was the primary mode of crack development observed during these tests. The initiation of first crack was always close to the centre of the layer in all three specimens. Kodikara and Choi (2006) have presented a theoretical background for this phenomenon based on the maximum stress that develops in a layer. According to their analytical model the maximum stress occurs at the centre of the layer thus facilitating the crack initiation. Then, sequential sub-division follows dividing each cracked cell into smaller cells. Time-laps video clips were produced from the testing.

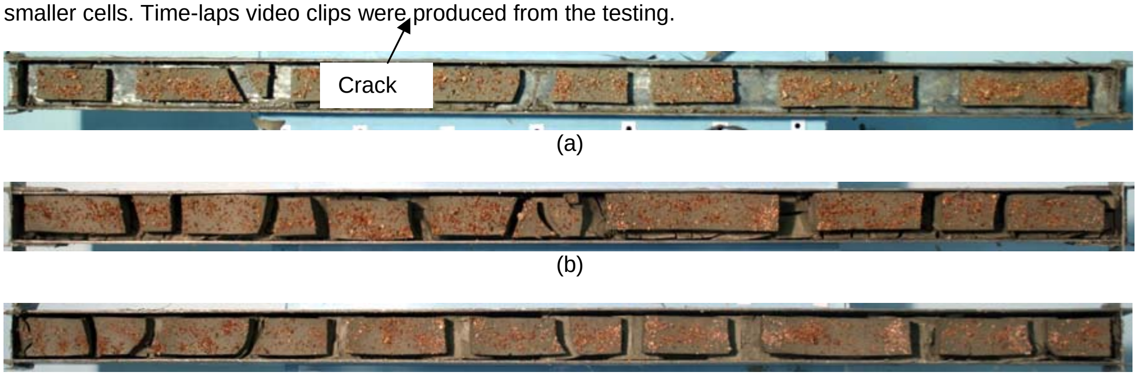

(a)

(b)

(c)

Figure 1. Final crack patterns in the three specimens (a) test 1, (b) test 2, (c) test 3

5.1 Crack initiation

The evolution of cracks is a vital stage of the cracking process from modelling perspective. Many researchers have attempted to develop models to predict crack initiation (e.g., Konrad and Ayad, 1997). Commonly used criterion is to consider that a desiccation crack is initiated when the tensile stress generated during drying exceeds the tensile strength of the material. However, the tensile strength of the material is a function of the original flaw distribution within the material. Therefore, the exact location of the crack initiation will depend on this flaw distribution as well, or alternatively, on the spatial distribution of the tensile strength. Subsequent fracture propagation is generally governed by the fracture energy of the material and the release rate of the strain energy accumulated during desiccation. However, during the desiccation process, all these parameters change with the decrease of moisture content.

We made use of the PIV technique to study the strain localization in the material at the crack initiation. A detailed description of an arbitrarily selected crack from test 2 is shown in Figure 2 as follows.

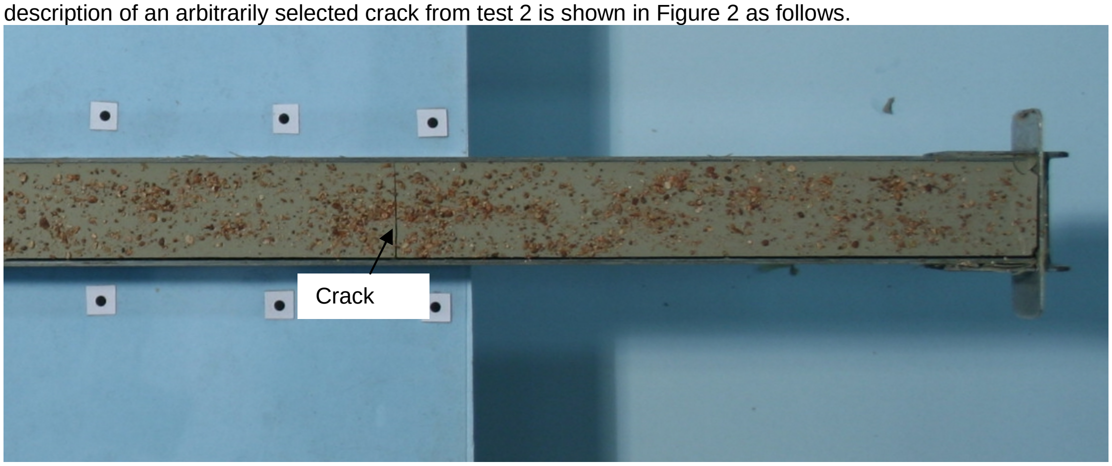

Figure 2. The crack from test 2, analysed in detail in Figure 3

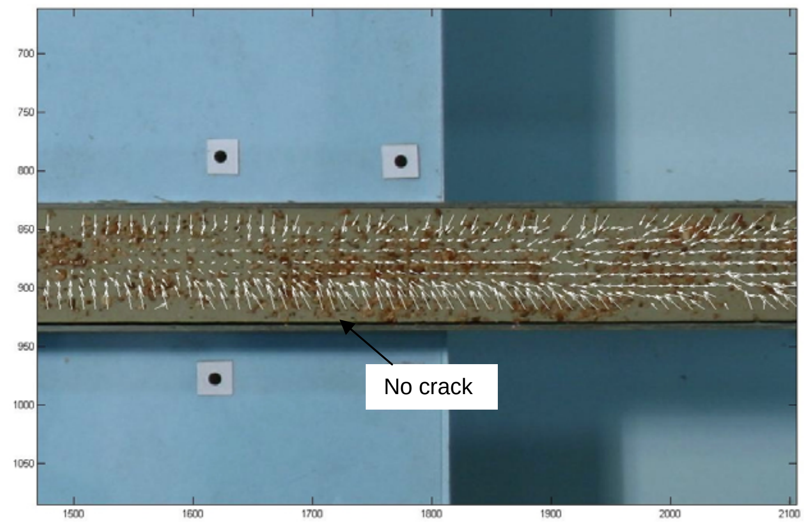
No crack
700
750
800
850
900
950
1000
1050
1500
1600
1700
1800
1900
2000
2100

(a)

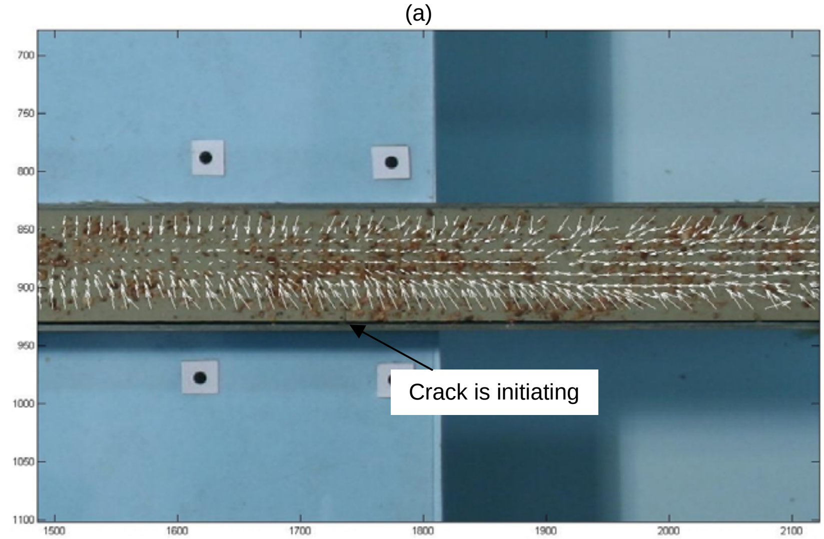
Crack is initiating
700
750
800
850
900
950
1000
1050
1100
1500
1600
1700
1800
1900
2000
2100

(b)

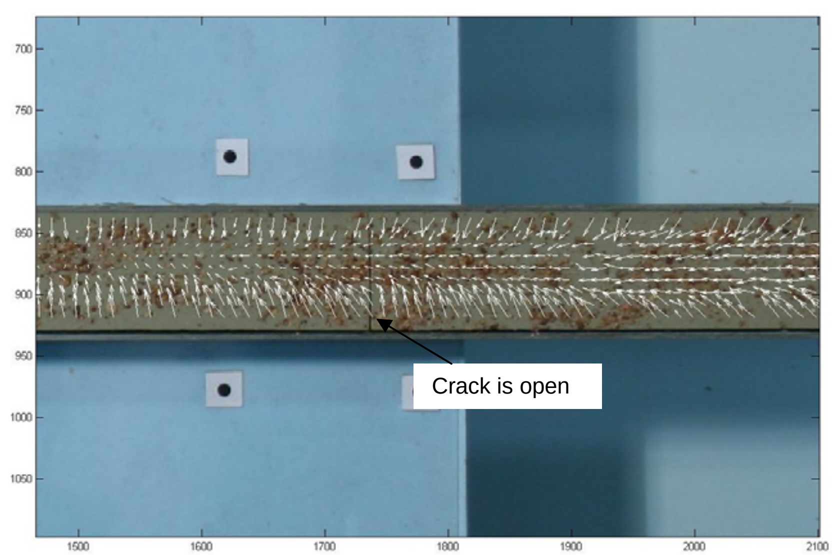
Crack is open
700
750
800
850
900
950
1000
1050
1500
1600
1700
1800
1900
2000
2100

(c)

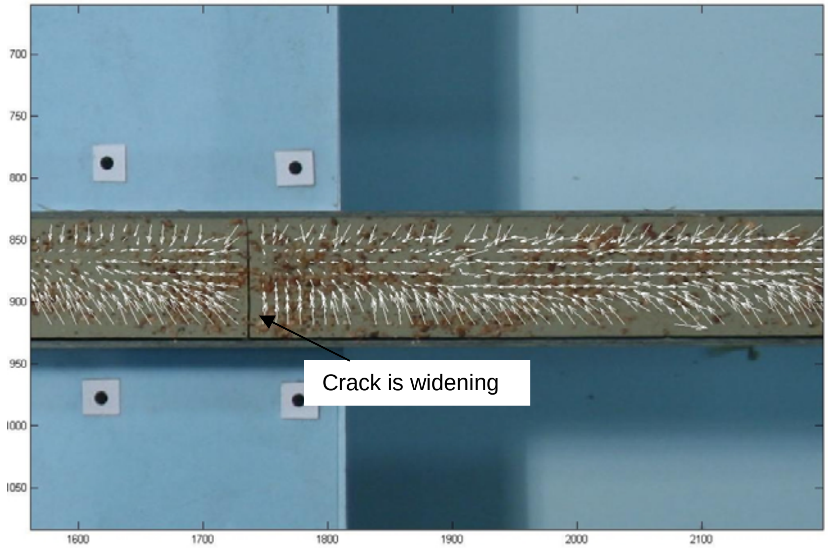

(d)
Figure 3. Strain contours at the crack initiation (a) No crack, (b) Crack is initiating (c) Crack is open, (d) Crack is widening

Figure 3 (a) – (d) present the displacement vectors at the proximity of the crack. Before the initiation of the crack as shown in Figure 3(a), the material is shrinking more in the lateral direction to the longitudinal direction. This was facilitated by having greased boundaries (but not the base). In the longitudinal direction, displacement vectors are of the same size except towards the left side, where the displacement vectors reduce to almost zero. Therefore, the observed strain is increasing towards the left side. Another observation is that the displacement in longitudinal direction is restrained because it is less than the lateral displacement considering that free shrinkage is mostly isotropic. This restraint is considered to arise primarily from the base adhesion for these relatively thin layers. Figure 3(b) shows the displacement vectors soon after initiation of the concerned crack. Strain contour plots show that there is strain localisation around this region, but it is not very clear. Figure 3(c) shows the displacement field after the extension of the crack almost full extent across the clay layer. Still overall displacement vectors are dominant not showing the influence of the crack on the surrounding displacement field. Figure 3(d) shows sometime after the crack has widened, and at this stage, the displacement field is showing the influence of the crack dynamics. While the crack is widening from the left side, the displacements on the right side next to the crack is almost halted. So the release of strain is almost towards the left side, at this stage, but with time, the crack extends from both sides.

Almost all the cracks were initiated at the early stage of the drying period. Most of them were opened up within the first few hours. Figure 4 illustrates the development of number of cracks with the drying time. Thicker specimens (test 3) tend to crack earlier than the thin specimens. As shown in Figure 4, once the first crack is initiated, the subdivision continues rapidly until the number of cracked cells reaches a maximum, beyond which cells continue to shrink but no further cracking occurs. The maximum number of cells, however, is likely to be a function of the parameters of the drying environment and basal adhesion characteristics (Kodikara and Choi, 2006).

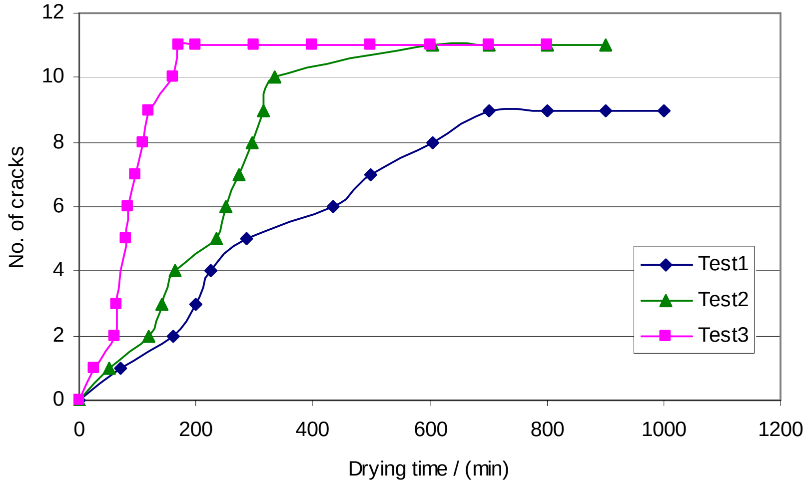

Figure 4. Development of number of cracks with drying time

5.2 Overall displacement fields

PIV software has the ability to produce displacement vector fields related to the soil movement, as discussed earlier. A Complete displacement vector field for the test 3 is given in Figure 5(a). The vectors indicate the soil movement within the cells, with Figure 5(c) showing displacement field for one of the cells in closer detail. It is clear that once cracks have initiated, the subsequent displacement fields depict more closely the isotropic shrinkage of the cells. This is an indication that the adhesion at the base has diminished with decrease of moisture, allowing cells to undergo shrinkage without too much restraints from the base adhesion.

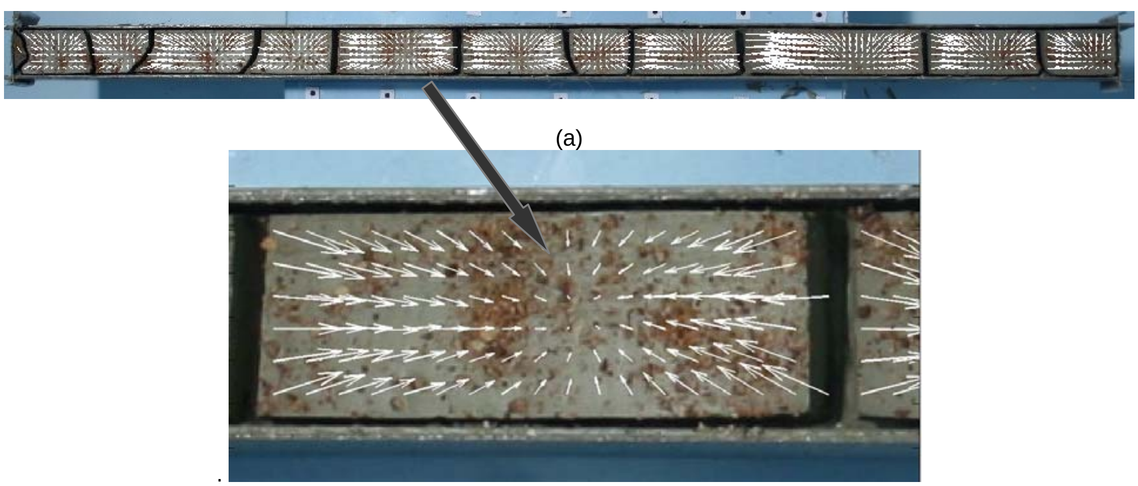

(a)

(b)

Figure 5. Displacement vectors for test 3 (a) displacement fields for all cells, (b) displacement field for one of the cells expanded, as shown.

5.3 Moisture loss and shrinkage strain

Figure 6 shows the relationship between the average linear shrinkage strain and the reduction in average moisture content determined from continuous weighing measurements. The average linear strain was computed by taking the total reduction of the length in each cell divided by the original length or the length of the mould. For both test 1 and test 2, almost linear relationships are obtained. Test 3 shows similar linear behaviour at the middle but deviates at the beginning and at the end. Peron et al. (2007) and Kodikara and Choi (2006) have also reported similar behaviour for clay soils. It should be noted, however, that the results shown in Figure 6 is for cracking tests, where strains may have been influenced by basal restraints. Kodikara and Choi (2006) presented similar results but for free shrinkage in Werribee clay. Their results gave a comparative gradient of 0.253, which compares well with that in Figure 6, despite the issue of possible restraints influencing the shrinkage strains during cracking. It should be noted that this gradient is very close to that calculated on the basis, $de = G_s dw$, where G_s is the specific gravity. This highlights that the material remains close to saturation during the crack development for clays drying from close to the liquid limit.

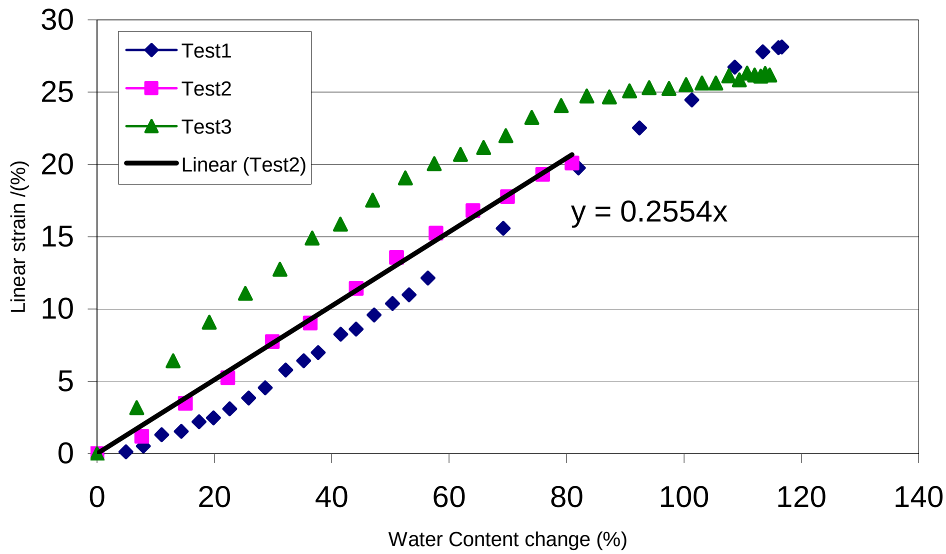

Figure 6. Average shrinkage strain with average water content change for cracking tests

6 Theoretical interpretation

The experimental observations have shown that that desiccating soil experiences certain observed (or mobilised) strain increment $(d\varepsilon_{ij})$ below a free isotropic linear shrinkage strain increment $(d\varepsilon_{sh})$ over a certain time increment. Tensile strains and stresses are assumed to be positive. Therefore, the constitutive relation for the desiccating soil can be written as (Peron et al, 2007; Kodikara and Choi, 2006):

$$d\sigma_{ij} = E_{ijkl}\left(d\varepsilon_{kl} - \delta_{kl} d\varepsilon_{sh}\right) \tag{1}$$

Where, E_{ijkl} is the tangent elastic stiffness tensor and $d\sigma_{ij}$ is the stress increment over time period considered, and δ_{kl} is Kronecker delta. The shrinkage strain increment can be related to moisture content reduction (dw) as:

$$d\varepsilon_{sh} = \alpha\, dw \tag{2}$$

Where α is the gradient of the free shrinkage strain and moisture loss, discussed earlier. Therefore, Equation (1) can be written as:

$$d\sigma_{ij} = E_{ijkl}\left(d\varepsilon_{kl} - \delta_{kl}\alpha dw\right) \tag{3}$$

Peron et al. (2007) presented how the above constitutive relation can be used with equilibrium equation to solve the desiccation of clay in long moulds up to first cracking. Their work, however, did not include the evolution of cracks. Kodikara and Choi (2006) presented a simplified approach to the above equations and produced predictions of evolution of cracks with time. The observations made in these experiments agree with previous observations that the number of cracks increase rapidly once cracking is initiated and then reaches a maximum value corresponding to the surrounding ambient conditions.

7 Conclusion

This paper presents particle image velocimetry (PIV) analysis to study the strain and displacement fields in desiccating soil layers in long moulds. The analysis indicated that initial shrinkage is highly anisotropic due to restraints for shrinkage in the longitudinal direction. While almost free shrinkage occurred in the lateral direction, which was facilitated by greasing of the edge walls of the mould, the observed longitudinal shrinkage was much less up to cracking due to restraints provided predominantly by the basal adhesion. This led to crack initiation with the development of tensile stresses. The crack development occurred with sequential subdivision of clay layers close to middle of each layer, but was apparently influenced by the dominant flaws in the material. It was found that even for cracked cells, the average shrinkage strain showed predominantly a linear relationship to the reduction in moisture content. It was shown that this observation provides a simplified way to model the desiccation process. It should be noted, however, that sometimes, cracks occurred very close to each other and not exactly in the lateral direction, showing that the cracking process is very sensitive to small variations of strength and stresses. This actually poses challenges to developing accurate numerical models. It is, however, not expected that numerical modelling will lead to exact prediction of the cracking locations, but attempt to provide a statistically similar crack pattern for moisture flow or hydro-mechanical interaction simulations.

8 Acknowledgement

The support given by Australian Research Council's Discovery Scheme is gratefully acknowledged. Thanks are also rendered to Ben Shannon who helped undertake some of the experiments.

9 References

Corte, A. and Higashi, A. 1960. Experimental research on desiccation crack in soil. U.S. Army Snow Ice and PermafrostResearch Establishment. Research report No.66. Corps of Engineers. USA.

Costa, S. M., Kodikara, J. 2007. Investigation of desiccation cracking using automated digital photography, Proc. 10th Australia New Zealand Conference on Geomechanics, Brisbane (Australia), 338-343.

Costa, M., Kodikara, J., Thusyanthan, N. I. 2008. Study of desiccation crack evolution using image analysis, 1st European Conference on Unsaturated Soils, Durham (United Kingdom), *Under review*

Deegan, R.D., Bakajin, O.,Dupont, T.F., Huber, G., Negal, S.R. and Witten, T.A.1997, Capillary flow the cause of ring stains from dried liquid drops, Nature, **389**, 827-829.

Kodikara, J.K., Barbour, S.L., Fredlund, D.G. 2000. Desiccation cracking of soil layers, Proceedings of Asian Conference on Unsaturated Soils: From Theory to Practice, Singapore 693-698.

Kodikara, J.K., Choi, X. 2006. A simplified analytical model for desiccation cracking of clay layers in laboratory tests, Proc. UNSAT2006 Conference, Arizona (USA), 2558-2567.

Konrad, J. M., Ayad, R. 1997. An idealized framework for the analysis of cohesive soils undergoing desiccation, Canadian Geotechnical Journal, 34, 477-488.

Lachenbruch, A. H. 1961. Depth and Spacing of Tension Cracks, Journal of Geophysical Research, **66**(12), 4273-4292.

Lakshmikantha, M.R., Prat, P.C. and Ladesma,A. 2006. An experimental study of cracking mechanisms in drying soils, Proc. 5th International Conference on Environmental Geotechnics, Thomas Telford, London.

Morris, P.H., Graham, J.and Williams, D. J. 1992. Cracking in drying soils, Canadian Geotechnical Journal, 29, 263-277.

Muller, G. 1998. Experimental simulation of basalt columns, J. Volcanology and Geothermal Research **86**, 93-96.

Nahlawi, H., 2004. Behaviour of reactive soil during desiccation, Masters Thesis, Monash University, Australia.

Nahlawi, H., and Kodikara, J.K. 2006. Laboratory experiments on desiccation cracking of thin soil layers, Journal of Geotechnical and Geological Engineering, GEGE2281, Springer Netherlands, **24**(6),1641-1664.

Peron, H., Hu, L.B., Laloui, L. and Hueckel, T. (2007). Mechanisms of desiccation cracking of soil: Validation, Numerical Models in Geomechanics – NUMOG X – Pande & Pietruszczak (eds), Taylor & Francis Group, London, ISBN 978-0-415-44027-1.

Thusyanthan, N. I., Take, W. A., Madabhushi, S.P.G., Bolton, M.D. 2007. Crack initiation in clay observed in beam bending, Ge´otechnique, **57**(7), 581–594.

White, D. J. 2002. An investigation into the behaviour of pressedin piles. PhD dissertation, University of Cambridge, UK.

White, D. J., Take, W. A. & Bolton, M. D. 2003. Soil deformation measurement using particle image velocimetry (PIV) and photogrammetry, Ge´otechnique, **53**(7), 619–631.

Yesiller, N., Miller, C. J., Inci, G., Yaldo, K. 2000. Desiccation and cracking behaviour of three compacted landfill liner soils, Engineering Geology, **57**, 105-121.